

WHAT CAN SKEWED REDUNDANT I.M.U. CONFIGURATIONS CONTRIBUTE TO PHOTOGRAMMETRY?

Ismael Colomina, Marc Giménez, José Rosales and Mariano Wis

Institute of Geomatics

Generalitat de Catalunya & Universitat Politècnica de Catalunya

Castelldefels, Spain

ABSTRACT

This paper discusses the possible application and benefits of redundant inertial measurement units to airborne photogrammetry and remote sensing (APRS). As the combination of Inertial Navigation Systems (INS) technology and the Global Positioning System (GPS) technology gains acceptance within the APRS community and as both the theory and the issues concerning their practical use become better understood one can start at looking at the technology and its context with a broader perspective. This paper presents preliminary studies on the feasibility of applying a geodetic/photogrammetric approach to the determination of INS/GPS trajectories; i.e. on the possible benefits of using redundant sensors (four or more pairs of gyroscopes and accelerometers). For this purpose, a test flight simulating a redundant configuration with two inertial measurement units has been conducted. The paper, in addition to theory for combining multiple inertial sensors, describes the flight and does a preliminary comparative analysis between the two data sets.

1 INTRODUCTION

With the exception of frame cameras —and any other 2D imaging sensor—, modern airborne photogrammetric and remote sensing sensors depend on inertial and satellite navigation technologies for their orientation. In the last five to ten years, the combination of these two technologies has ranged from useful to essential depending on the sensor imaging geometry. Typically, a medium frequency (50-400 Hz) set of inertial observations is integrated with a low frequency (1-10 Hz) set of GPS observations. Usually, in post-processing, orientation is obtained from these data in three steps. (Orientation is here understood as both positioning and attitude determination.) First, the low frequency GPS trajectory is generated. In a second step, a Kalman filter and smoother is used to densify and smooth the GPS trajectory with the inertial observations. The result is the so-called INS/GPS trajectory. Then, in a later step the INS/GPS trajectory position and attitude data is interpolated to the sensor exposure times and transferred to the sensor reference frame.

The combined INS/GPS technology delivers orientation at precision and accuracy levels sufficient for most —if not every— APRS application. Interestingly enough, the main objections and difficulties in the application of inertial technology to APRS originate from the limitations of GPS and from the limitations of the APRS sensors. GPS was not designed to fulfill the demanding requirements of APRS and, up to few years ago, many APRS sensors were not designed with INS/GPS in mind. GPS has, for the APRS applications, too few satellites and too few signals. And many APRS sensors do not allow for an easy, reliable and time stable transfer of attitude from the inertial measurement unit (IMU) instrumental reference frame to the sensor instrumental reference frame.

Say what you will about the performance of such or that particular INS/GPS system, but most INS/GPS tests have been rather a test on attitude transfer than on INS/GPS performance. No wonder that this was the case, since the inertial navigation technology itself is a highly developed, mature discipline, older than GPS and aerial triangulation, standing on large investments on research, development, testing, large scale manufacturing and daily operation.

The above situation and the subsequent research, development and operation efforts have dominated the scene for the past few years (Colomina, 1999). However, as new APRS sensor designs are being fielded and the attitude transfer stability problem is being confined to the analogue metric cameras, other issues in the pipeline are emerging. One of them is the development of a true geomatic —call it geodetic or photogrammetric if you wish— algorithmic approach to the analysis and processing of inertial, GPS and photogrammetric data; for the approach used so far was a navigation algorithmic approach based on [non redundant] sets of three plus three inertial observations which, at epochs of GPS availability, undergo calibration. Bad luck, of course, if there are periods without GPS information! Certainly, this is not the case for APRS. However, for the emerging terrestrial mobile mapping applications, GPS outages and signal multipath are the biggest problems.

(To be fair to navigation, it has to be said that actual navigation practices are extremely safe and redundancy based. However, the redundancy is rather at the system level than at the algorithmic level. Thus, for instance, in civil air aviation,

airliners are equipped with three inertial navigation systems. The various INS, however, are independent from each other and each INS operates on non redundant observations.)

A key characteristic of the geomatic methodology is the design of measurement devices and campaigns with sufficient redundancy and adequate configuration. In this paper first investigations on the use of redundant inertial sensors in IMUs for APRS applications are reported. The possible benefits of such an approach can be, among others, the following: actual noise estimation for precision improvement; systematic or deterministic error modeling for accuracy improvement; stochastic error modeling for accuracy improvement; failure detection and isolation for reliability and integrity improvement; and resilience to single sensor malfunctioning for robust operations and their logistics. If this is the case—and this is not yet claimed but just hypothesized—other benefits like realistic noise estimation under various vehicle dynamics, fast IMU error modeling and mitigation of the larger heading drift may be expected.

2 SKEWED REDUNDANT IMU CONFIGURATIONS

As already mentioned, the use of redundant inertial sensors is not new. In general terms, the recent availability of low cost, low weight, low power consumption sensors has been instrumental in the development of the sensor network concept. Therefore, not only the concerns on the lack of a geodetic approach but also the possibility to benefit from non expensive redundant configurations, justify that some attention is paid to the issue.

There are multiple architecture topologies that combine inertial sensors in various ways. This paper focuses on a configuration known as skewed redundant IMU (SRIMU). A SRIMU configuration is a non-orthogonal IMU configuration with respect to the aircraft body axes or with respect to the three orthogonal axes on an imaginary IMU within the SRIMU.

Assume then, that there exists a SRIMU with $2n$ sensors; n gyroscopes and n accelerometers, where $n > 3$. Assume further, that the inertial observations from the SRIMU are

$$\ell^b = \begin{pmatrix} \ell_\omega^b \\ \ell_a^b \end{pmatrix}$$

where ℓ_ω^b contains the n angular velocity observations and ℓ_a^b the n linear acceleration observations.

Assume, as well, that the SRIMU manufacturer has carefully crafted and calibrated the unit, so that the axes of the various accelerometer/gyroscope pairs¹ are well known in some instrumental “body” reference frame b . Then, the following equation could be established

$$\begin{pmatrix} \ell_\omega^b \\ \ell_a^b \end{pmatrix} = \begin{bmatrix} A & 0 \\ 0 & A \end{bmatrix} \begin{pmatrix} \omega_x^b \\ \omega_y^b \\ \omega_z^b \\ a_x^b \\ a_y^b \\ a_z^b \end{pmatrix}$$

where A is a $n \times 3$ matrix which contains the geometry of the SRIMU and the vector $(\omega_x^b, \omega_y^b, \omega_z^b, a_x^b, a_y^b, a_z^b)^T$ is the vector of what could be called a synthetic or virtual IMU.

The interesting thing about the above matrix equation is that it allows for the computation of a realistic, epoch by epoch, covariance matrix of the inertial synthetic observations. For this purpose, it suffices to perform two independent least-squares adjustments for the determination of the best estimates of $\omega^b = (\omega_x^b, \omega_y^b, \omega_z^b)^T$ and $a^b = (a_x^b, a_y^b, a_z^b)^T$. Then, through the estimation of the two corresponding variances of unit weight, two realistic estimates

$$C_{a^b a^b} = \widehat{\sigma_{a_0}^2} \left(A^T C_{\ell_a^b}^{-1} A \right)^{-1} \quad \text{and} \quad C_{\omega^b \omega^b} = \widehat{\sigma_{\omega_0}^2} \left(A^T C_{\ell_\omega^b}^{-1} A \right)^{-1}$$

of the quality of the synthetic inertial data can be easily obtained. The variance factors $\widehat{\sigma_{a_0}^2}$ and $\widehat{\sigma_{\omega_0}^2}$ are computed in the usual way from the residuals of the least squares estimation.

An advantage of this approach is that it allows to use existing INS or INS/GPS software packages without any modification other than generating a synthetic input inertial data set. Of course, the INS software should allow for an independent, time dependent, weighting of the inertial observations.

¹Rigorously speaking, a redundant inertial configuration does not require an equal number of accelerometers and gyroscopes. It could even be just redundant for the accelerations or just redundant for the angular velocities.

Another slightly different approach consists in using the $2n$ redundant inertial observations in extended INS mechanization equations. In the following formulation the well known INS mechanization equations (see (Savage, 1998a, Savage, 1998b), for instance) parametrized in cartesian geocentric coordinate system. To further illustrate the situation with calibration states, biases following a first order Gauss-Markov model have been introduced. The modified equations turn out to be

$$\begin{aligned}\dot{x}^e &= v^e \\ \dot{v}^e &= R_b^e \Pi (\ell_a^b + a^b) - 2\Omega_{ie}^e v^e + g^e(x^e) \\ \dot{R}_b^e &= R_b^e (\Omega_{ei}^b + \Omega_{ib}^b + \Omega^b(o^b)) \\ \dot{o}^b &= -\beta o^b \\ \dot{a}^b &= -\alpha a^b\end{aligned}$$

where Ω_{ib}^b , —a well known matrix in the INS world— is a skew symmetric matrix

$$\Omega_{ib}^b = \begin{pmatrix} 0 & -\omega_z & \omega_y \\ \omega_z & 0 & -\omega_x \\ -\omega_y & \omega_x & 0 \end{pmatrix}$$

that, in the SRIMU case, is built by substituting the variables ω_x^b , ω_y^b and ω_z^b by the expressions derived from

$$\begin{pmatrix} \omega_x^b \\ \omega_y^b \\ \omega_z^b \end{pmatrix} = \Pi \ell_\omega^b,$$

where the dimensions of the calibration vectors o^b and a^b are n , and where Π is a $3 \times n$ orthogonal projector

$$\Pi = \left(A^T C_{\ell_\omega^b, \ell_\omega^b}^{-1} A \right)^{-1} A^T C_{\ell_\omega^b, \ell_\omega^b}^{-1}.$$

This second approach, allows for the direct calibration of each of the original redundant sensors. The calibration can be performed in the usual way, at epochs when external information is available. But it can also be performed continuously, at the rate of the inertial observations, by exploiting the redundancy of the inertial data itself. Moreover, this is necessary for the realistic error estimates of the inertial redundant observations. (See (Allerton and Jia, 2002) for a similar treatment for SRIMU calibration and modeling.)

3 THE TEST FLIGHT

In order to simulate a SRIMU, two Northrop Grumann (formerly Litton) LN-200 inertial units were fixed to a Zeiss RMK TOP camera on a Cessna 207 Stationair airplane. One unit, was the LN-200 IMU from an Applanix POS/AV 410 system (Scherzinger, 1997). This tactical, 1 deg/h, fiber optic gyro unit delivers linear accelerations and angular velocities at 200 Hz. Both the IMU and the airplane are owned by the company HIFSA, in Madrid, Spain. The second unit, owned by the Institute of Geomatics (IG), is, as well, a Northrop Grumann LN-200 whose output rate is 400 Hz. With the exception of the output rate, to the knowledge of the authors, both IMUs share the same technical specifications. The IG's LN-200 is controlled by the experimental TAG system ((Wis and Colomina, 2003) and (Wis et al., 2003)). The two IMUs will be referred to as the STO and the TAG IMU respectively. During the flight, inertial data were collected simultaneously and independently by the STO and the TAG. The two data streams —the STO and the TAG— were synchronized through the common use of the GPS time reference scale defined by the GPS receiver 1 Hz pulses.

The relative attitude between the IMUs was selected to simulate a skewed redundant IMU of 6+6 sensors. The situation is depicted in figure 1. (The authors are aware that due to the IMU-to-IMU lever-arm, the two IMUs are sensing slightly different accelerations. However, for the purposes of the preliminary analysis presented in the paper, the accelerations differences can be neglected. In future, if necessary, they can be corrected.)

The test flight took place on 2003-07-01 in the vicinity of Robledo de Chavela, close to the NASA Deep Space Tracking Installation that has an IGS GPS permanent receiver (MADR). Weather conditions during the flight were very turbulent. The flight is composed of six strips following a typical photogrammetric flight pattern (see figure 2). Flying altitude ranged between 1700 and 2200 meters and flying speed was about 220 km/h.

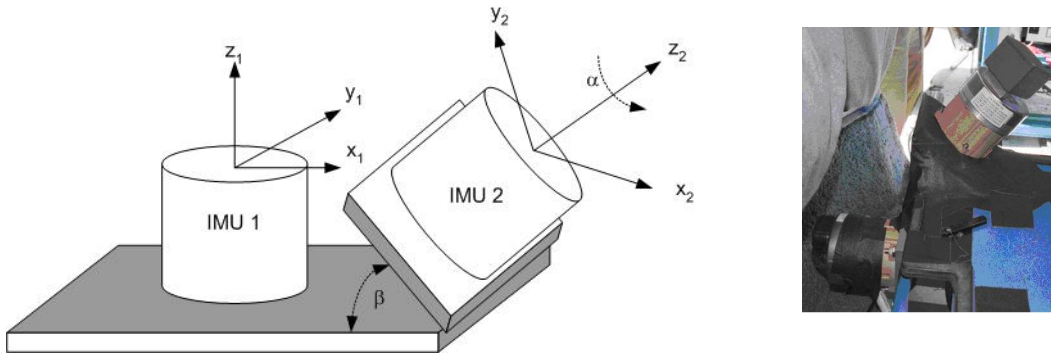


Figure 1: Schematic layout and photograph of the dual IMU flight test setup.

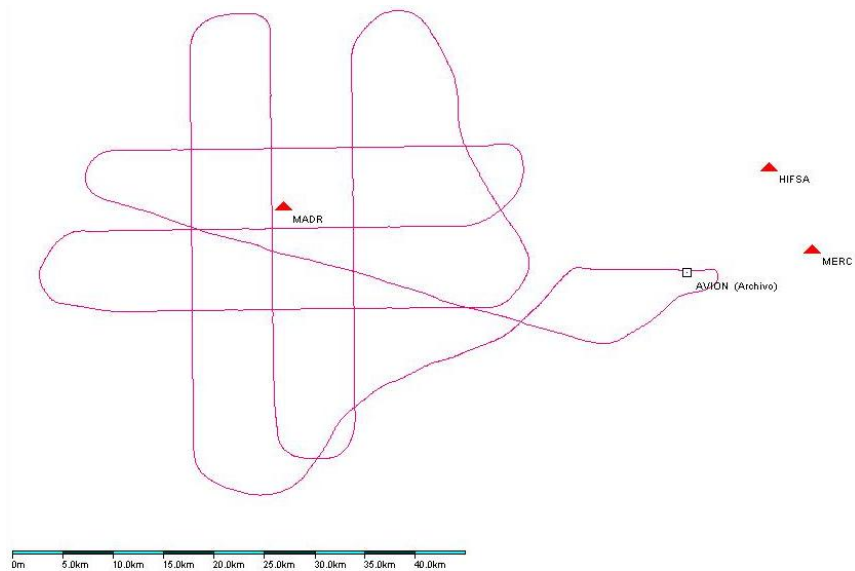


Figure 2: Test flight path, GPS reference stations and airport base.

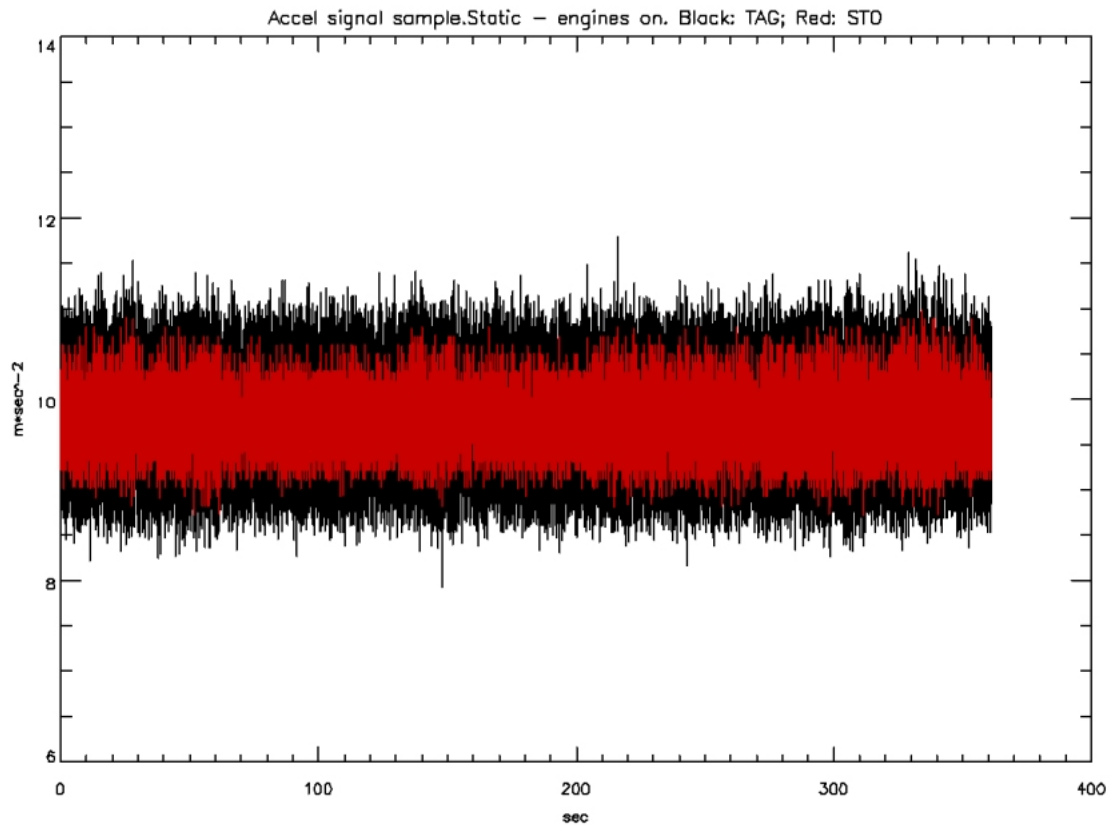


Figure 3: Acceleration signal from both STO (LN-200 at 200 Hz, red) and TAG (LN-200 at 400 Hz, black) units. (Airplane static - engines on.)

4 PRELIMINARY RESULTS

In the sequel, preliminary results obtained from the experiment described in section 3 are discussed. The frequency response of the accelerometers and the gyroscopes of both IMUs has been analysed in two different situations: airplane static with engines on (“static-engines on” case) and airplane flying (“kinematic” case). In addition to this, a similar analysis for time period of true static observation of the TAG has been included for comparison purposes and to check the consistency of the captured data.

4.1 Analysis of the “static-engines on” case

In this case a 6 minutes signal interval from the accelerometers and the gyroscopes have been studied. In order to easily compare the signals from both IMUs the module of the accelerometer vector observation and the module of the gyroscope vector observation have been considered.

In the case of the accelerometers, the result signal from both IMUs can be seen in figure 3. It can be observed that the TAG signal is noisier than the STO signal. This is according theory predictions because the different sampling rates of the two IMUs. Internally, both IMUs generate data at 2000 Hz but they have different average intervals (5 samples for the LN-200 at 400 Hz and 10 samples for the LN-200 at 200 Hz). The shorter the averaging is, the higher the noise is. In this particular case, a $\sqrt{2}$ factor is just a rough approximation of reality because of the presence of quiescent noise due to the airplane engines. This quiescent noise can be easily seen in figure 4. The figure depicts the Fourier Transform (FFT) of the 6 minutes interval acceleration signal of the two IMUs. This frequency plot is shown from 0 Hz to 100 Hz because of the STO 200 Hz rate. The 200 Hz spectrum of the TAG is analyzed later within this section.

In figure 4, it can be seen that the vibrations of the airplane structure induced by the engines dominate the signal from 0 to 20 Hz. From 20 Hz to 70 Hz, the STO signal is slightly noisier than the TAG signal. Beyond this frequency, the TAG signal is stronger and increases until the end of the interval. In the 70 Hz to 100 Hz interval, the TAG signal is noisier than the STO signal.

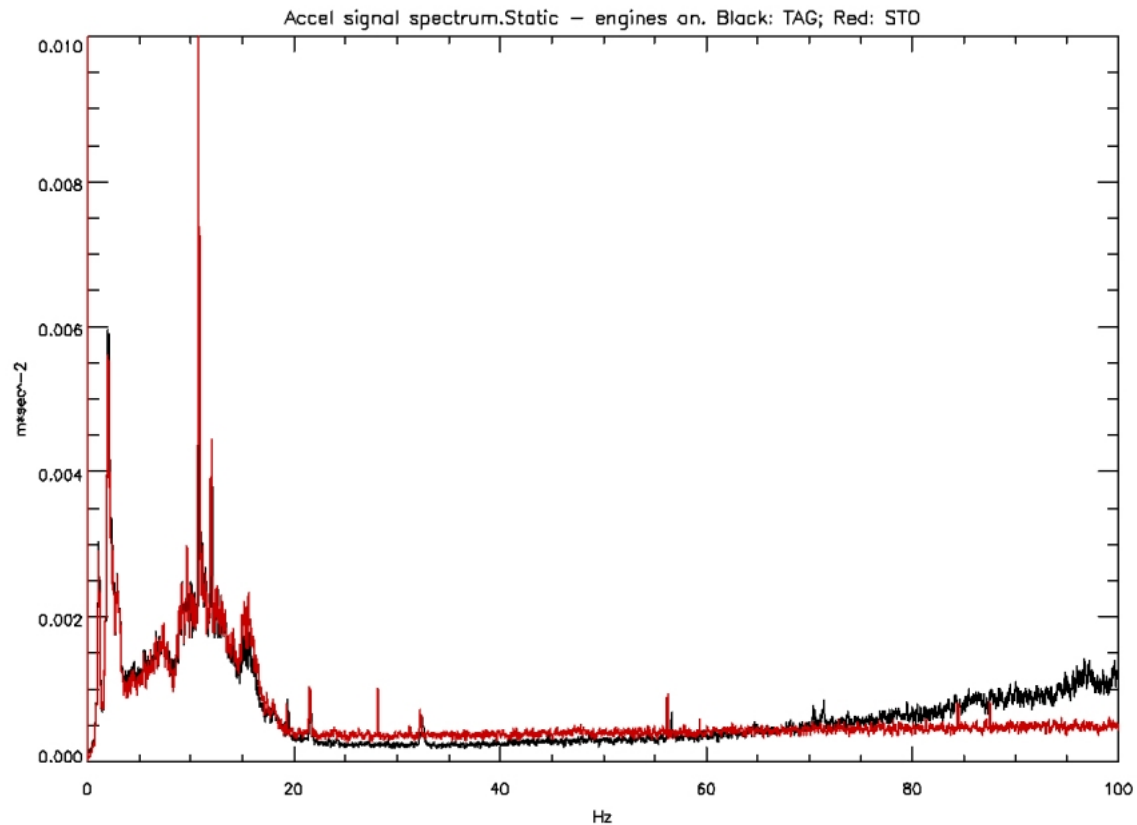


Figure 4: Acceleration signal spectrum from both STO (LN-200 at 200 Hz, red) and TAG (LN-200 at 400 Hz, black) units. (Airplane static - engines on.)

A similar procedure has been applied to the gyroscopes signal and their spectra (figures 5 and 6). In this case, the “noise” induced by the engines can be regarded as signal for both sensors. To illustrate the similarity between both signals, an interval of 5 seconds has been used in both figures. When analyzing the spectra of both signals (figure 6), it can be seen that the only difference are small slopes beyond 70 Hz.

4.2 Analysis of the “kinematic” case

In this case, the signal is obviously reflecting the noise of the sensors, the vibrations of the engines and the vehicle motion. A small interval of accelerometers and gyros’ signals can be seen in figure 7. As expected and in accordance with theory, the high frequency signals (TAG) are a bit noisier than the low frequency ones (STO). When comparing the spectra of both signals, (figure 8) it can be seen that flight motion dominates within the 20 Hz to 30 Hz frequency band. Some strong peaks can be observed around 20 Hz, 40 Hz and 60 Hz frequencies, probably due to influence of engines’ vibrations and turbulences on the plane frame. Again, it can be seen that the TAG sensors are a bit noisier for frequencies higher than 70 Hz.

4.3 Final data consistency analysis

In this section, a comparative analysis of spectra is performed, to show that the TAG and the STO data sets are consistent. In figure 9, the spectra for the true static case, for the static case with airplane engines on, and for the kinematic case are plotted. The effects of motion and vibrations can be observed. Booth for the accelerometers and the gyros, it can be seen that the spectra coefficients beyond the band 30 Hz - 40 Hz, are significantly larger in the kinematic case than in the static-engines on case. In addition to this, the spectra of the accelerometers and gyroscopes of the TAG IMU in strict static conditions are observed. (This static data was obtained in a different test performed at the Institute’s laboratory). Note, as well, the peak at the natural frequency of the accelerometers (about 130 Hz).

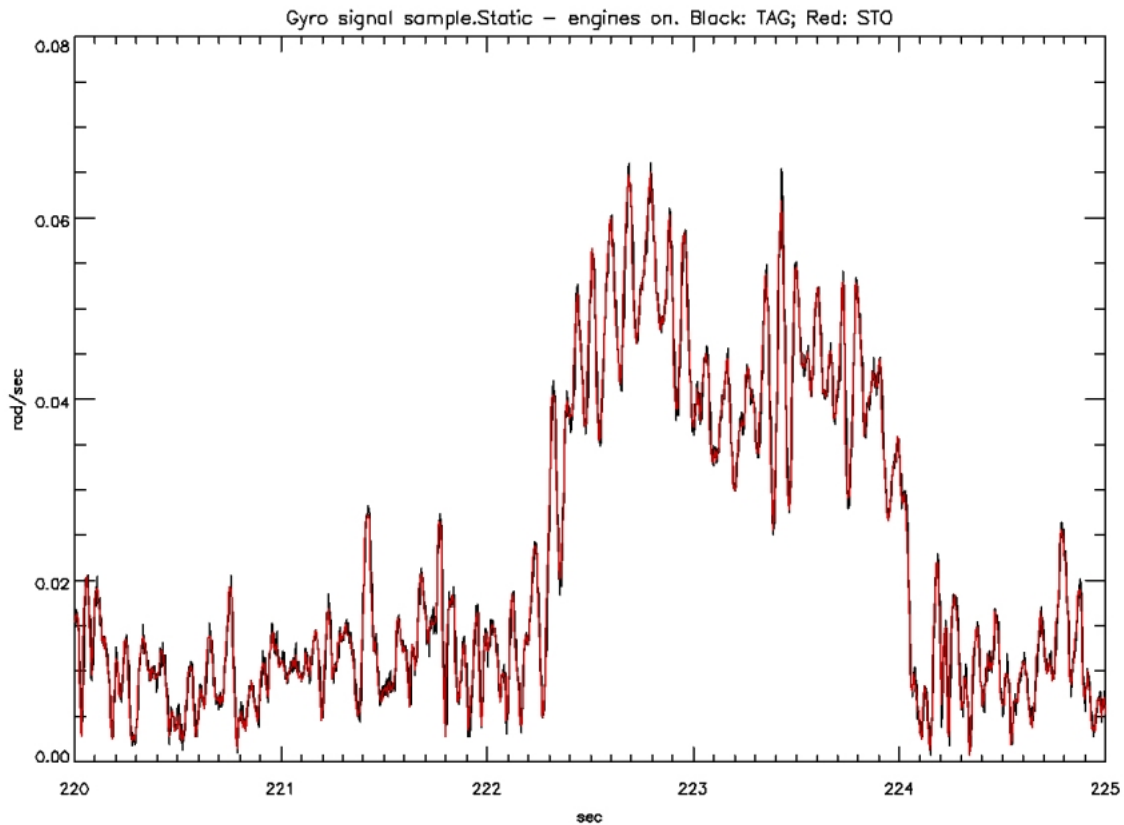


Figure 5: Angular velocity signal from both STO (LN-200 at 200 Hz, red) and TAG (LN-200 at 400 Hz, black) units. (Airplane static - engines on.)

A similar situation is encountered in figure 10 when analyzing the STO spectral data. The coefficients of the accelerometers spectra are larger under vibration and motion. The coefficients of the gyroscopes spectra exhibit the same behaviour in the band from 30 Hz to 70 Hz. Beyond 70 Hz, it seems that the spectra is describing noise.

The relevant conclusion of this section is that the two data sets are consistent and that the TAG data are noisier than the STO data, as expected. It makes sense, then, to further pursue the research effort and, in particular, to compute the rotation matrix from the TAG frame to the STO frame so that a synthetic, integrated, data set can be computed as described in section 2.

5 FINAL DISCUSSION AND WORK IN PROGRESS

In this paper the concept of redundant IMUs, their possible application to geomatics and related preliminary analysis on experimental data have been presented. (The concept of redundant IMUs is not new but, to the best knowledge of the authors, its application to geomatics is.) Procedures for the use of redundant inertial observations in the mechanization equations have been outlined together with a proposal for the correct estimation of the observations noise.

A test flight with two IMUs in a relative oblique position, thus simulating a skewed redundant IMU, has been conducted in order to assess the feasibility of the concept and to evaluate its performance. A description of the flight and its preliminary results have been presented and discussed.

The dual IMU data set has been analyzed for consistency by means of spectral analysis under various dynamic conditions and the first results indicate that these can support further research of the topic at the IG.

Future research with this data set will include the following items.

- The determination of two independent trajectories for each IMU.
- The generation of a synthetic standard IMU data set (combined inertial observations and their estimated covariance matrix) from the measured dual data set.

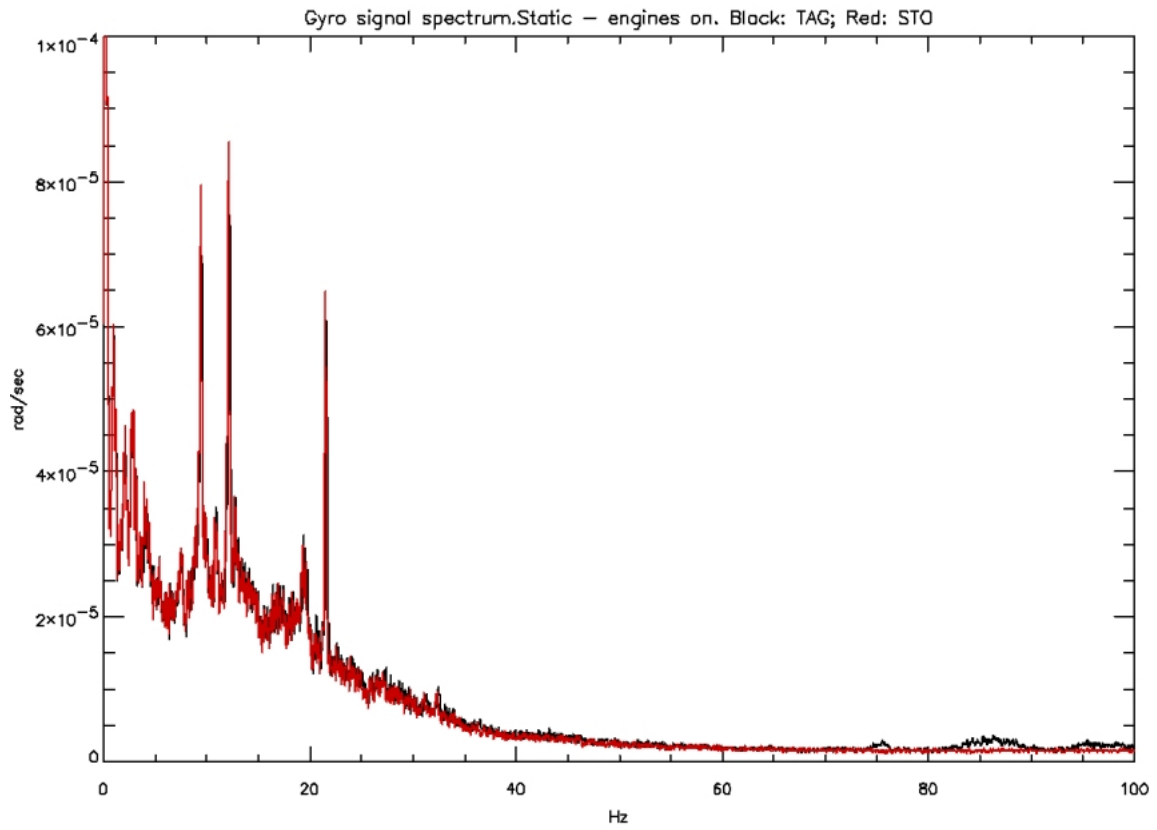


Figure 6: Angular velocity signal spectra from both STO (LN-200 at 200 Hz, red) and TAG (LN-200 at 400 Hz, black) units. (Airplane static - engines on.)

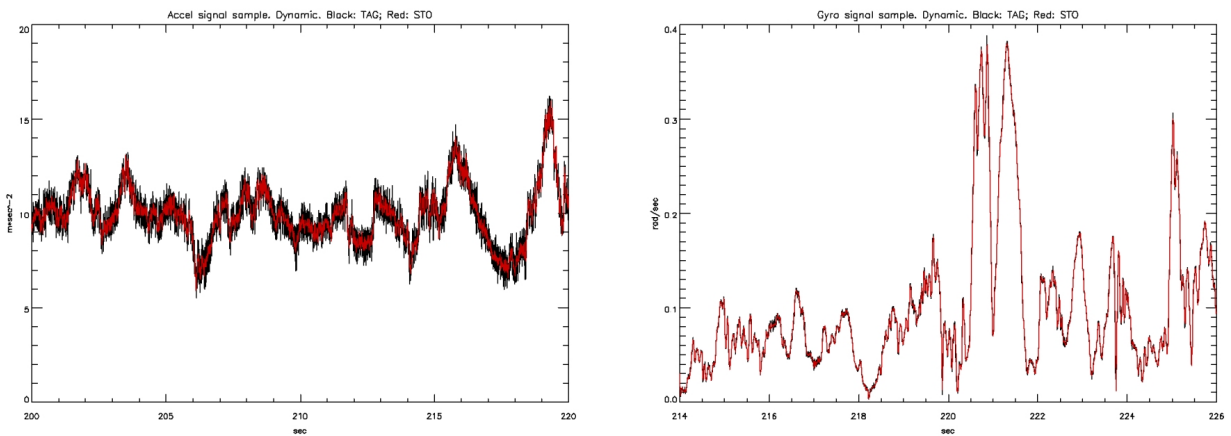


Figure 7: Acceleration and angular velocity signal from both STO (LN-200 at 200 Hz, red) and TAG (LN-200 at 400 Hz, black) units. (Airplane flying.)

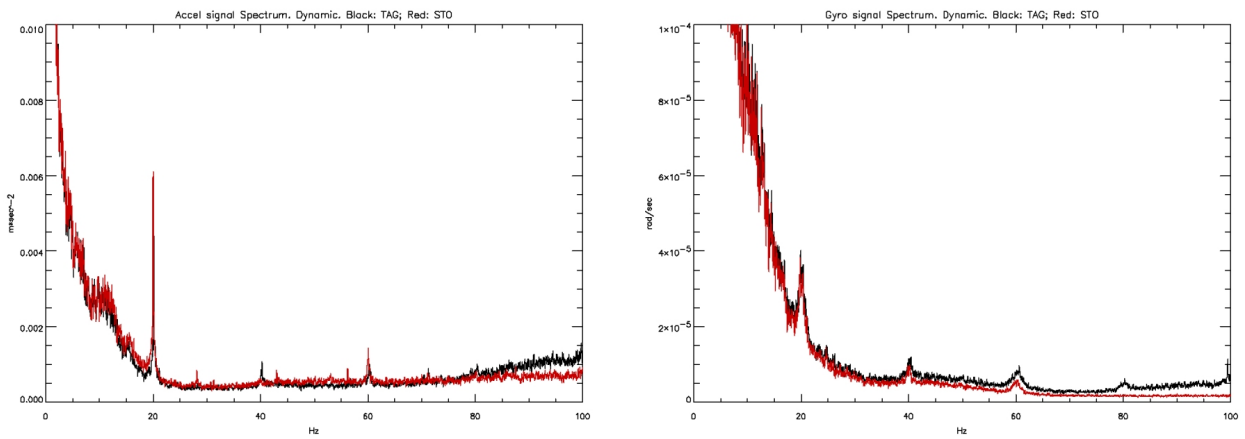


Figure 8: Acceleration and angular velocity spectra from both STO (LN-200 at 200 Hz, red) and TAG (LN-200 at 400 Hz, black) units. (Airplane flying).

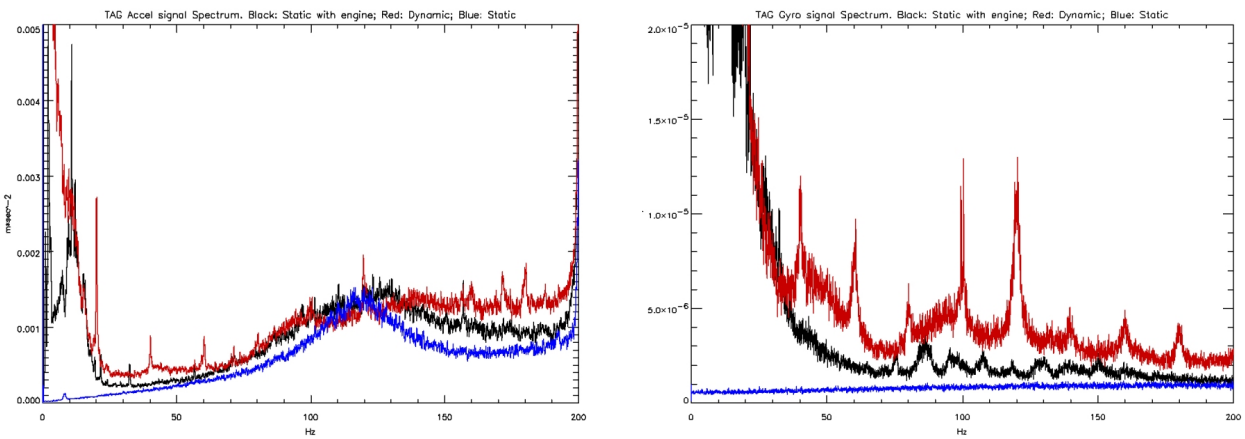


Figure 9: Acceleration and angular velocity spectra from the TAG unit (LN-200 at 400 Hz) unit. In red the "kinematic" case, in black the "static-engines on" case, in blue the "static-engines off" case.

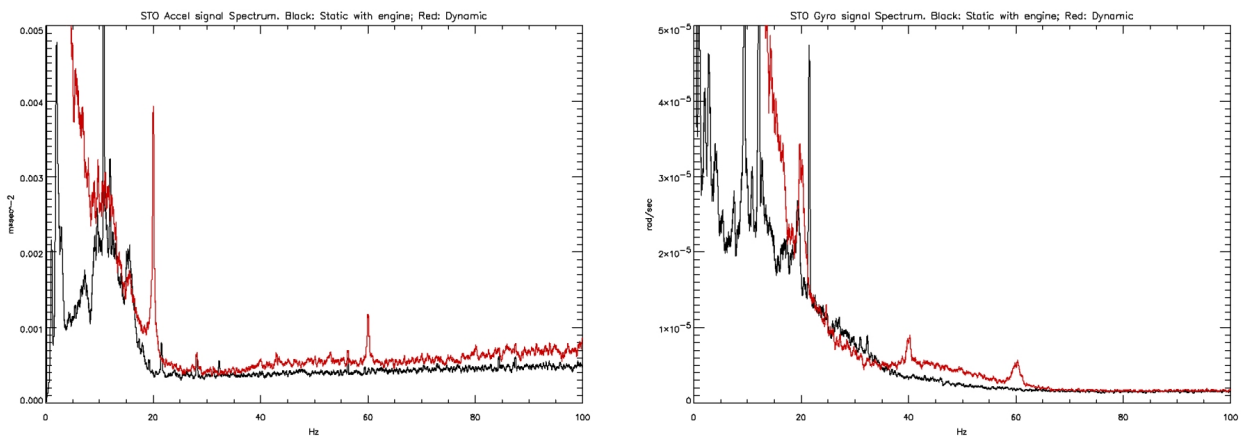


Figure 10: Acceleration and angular velocity spectra from the STO unit (LN-200 at 200 Hz) unit. In red the "kinematic" case, in black the "static-engines on" case.

- The determination of a trajectory for the synthetic IMU data set and its comparison with the two independent ones.
- The modification of the INS trajectory determination software to allow for the direct processing of the original dual data set. This modification affects both the INS mechanization equations and the filter.
- The observability analysis of the calibration states.
- The reliability (ability to detect errors and estimate their impact) of the redundant configurations, both theoretically and empirically after introducing deliberate errors in the data.
- The particular benefits of MEMS based SRIMU configurations.

What can skewed redundant IMU configurations contribute to photogrammetry? Certainly, improvements in various aspects like precision, accuracy and reliability are to be expected, as discussed in the preceding sections. However, the key question still to be answered is how significant these improvements are. With the available data set, the proposed agenda and with a controlled test flight the authors expect to do so.

6 ACKNOWLEDGEMENTS

The test flight was conducted by the StereoCARTO and HIFSA companies. The authors thank the cooperation of Dr.A.Gómez, Mr.M.A.Gómez-Aguado and Mr.P.Miguelsanz in its coordination, preparation and realization phases. The authors acknowledge, as well, the contribution of Ms.L.Samsó (IG) in the development of the TAG INS/GPS data acquisition system.

The research reported in this paper has been partially supported by the Spanish Ministry of Science and Technology, through the OTEA-g project of the the Spanish National Space Research Programme (reference: ESP2002-03687).

REFERENCES

- Allerton, D. and Jia, H., 2002. An error compensation method for skewed redundant inertial configuration. In: Proceedings of the ION 58th Annual Meeting and CIGTF 21st Guidance Test Symposium, Albuquerque, NM, USA, pp. 142–147.
- Colomina, I., 1999. GPS, INS and Aerial Triangulation: what is the best way for the operational determination of photogrammetric image orientation? In: International Archives of Photogrammetry and Remote Sensing, ISPRS Conference *Automatic Extraction of GIS Objects from Digital Imagery*, Vol. 32, München, pp. 121–130.
- Savage, P., 1998a. Strapdown inertial navigation integration algorithm design - part 1: attitude algorithms. *Journal of Guidance, Control and Dynamics* 21(1), pp. 19–28.
- Savage, P., 1998b. Strapdown inertial navigation integration algorithm design - part 2: velocity and position algorithms. *Journal of Guidance, Control and Dynamics* 21(2), pp. 208–221.
- Scherzinger, B., 1997. A position and orientation post-processing software package for inertial/GPS integration (POSPROC). In: Proceedings of the KISS'97 Symposium, Calgary, pp. 197–204.
- Wis, M. and Colomina, I., 2003. TAG: el sistema experimental de captura de datos de navegaci3n del IG. In: Proceedings of the 5. Geomatic Week, Barcelona.
- Wis, M., Colomina, I., G3mez, A., Andrinal, P. and Sanz, P., 2003. SEIRA: Sistema de Explotaci3n de Im3genes, R3pido y Aerotransportado. In: Proceedings of the 5. Geomatic Week, Barcelona.